Coloration Phenomenon of Mefenamic Acid in Mesoporous Silica FSM-16

Kunikazu Moribe,*[,a] Ryo Kinoshita,[a] Kenjirou Higashi,[a] Yuichi Tozuka,[b] and Keiji Yamamoto[a]

[a] *Graduate School of Pharmaceutical Sciences, Chiba University; 1–33 Yayoi-cho, Inage-ku, Chiba 263–8522, Japan: and* [b] *Laboratory of Pharmaceutical Engineering, Gifu Pharmaceutical University; 5–6–1 Mitahora-higashi, Gifu 502–8585, Japan.* Received September 18, 2009; accepted November 9, 2009; published online November 16, 2009

Coloration of mefenamic acid (MFA) was investigated in the presence of mesoporous silica FSM-16 with 16.0 Å (Oc) and 45.0 Å (Doc) pore diameter. The color change of MFA/FSM-16 physical mixture from white to deep blue was observed by sealed-heating (SH) and the subsequent humidification (HU). The coloration and the color difference were caused by the changes of chroma and lightness. In the case of MFA/FSM-16 (Oc), coloration was not observed by SH treatment only. Powder X-ray diffraction data indicated that difference of the dispersed states of MFA molecules in FSM-16 mesopore affected the coloration. MFA adsorbed on the silica surface and MFA in the mesopore were differentiated by thermogravimetric analysis. Solid-state ^{13}C-NMR showed that the molecular mobility of MFA was increased in the dispersed state in FSM-16 mesopores compared to the crystalline state. Structural changes of silanol groups in FSM-16 by humidification were observed by solid-state ^{29}Si-NMR. MFA adsorption in FSM-16 mesopore by SH as well as changes of the surface state of FSM-16 by HU affected the coloration of MFA.

Key words coloration; mesoporous silica; mefenamic acid; sealed heating; solid-state NMR

Large number of coloration studies has been reported. Most of the study was focused on inorganic materials,[1,2] dye and pigment.[3—5] Among the coloration phenomena, reversible one is named as suffix-chromism. Thermochromism[1] and mechanochronism[6,7] are the examples of reversible coloration.

Concerning the active pharmaceutical ingredients, coloration by photodegradation and hydrolysis during the storage has been reported.[8] Reversible coloration without chemical degradation may occur during a pharmaceutical processing.[6,9] Sheth *et al.* reported that coloration of piroxicam occurred by proton transfer to form the different charged states: neutral, charged and twitterionic. The unexpected coloration should be avoided by changing the formulation or using different unit process when it is due to the chemical reaction between a drug and an excipient or the degradation of a drug itself. When coloration is caused by intermolecular interaction among the components without chemical reaction, it does not affect the quality of drug. However, coloration of product is not preferred even if it is a reversible reaction.

Coloration of solid materials is usually occurred by specific absorption of visible light. The compensate color can be perceived from the eye as a color of the materials. Coloration of organic compounds depends on the presence of specific structure, such as chromophores and auxochromes including conjugated double bonds. Drugs can change the color when wavelength of the absorption peak shifts or a new absorption peak appears through intermolecular interaction with other excipients, even the drugs intrinsically show white color. Since reversible coloration usually disappears when the sample is dispersed or dissolved in solution, physicochemical characterization on solid state is a requisite to know the coloration mechanism. Conventionally used experimental apparatus are powder X-ray diffraction, thermal analysis and vibrational spectroscopic techniques, such as IR, near IR, and Raman spectroscopy. Recently, solid state NMR measurement becomes promising tool to evaluate the molecular states.[10—12] Appropriate measurement condition and method have to be selected to evaluate molecular mobility and states of materials precisely.

In this study, we investigated coloration phenomenon of mefenamic acid in mesoporous silica FSM-16 prepared by sealed-heating and the subsequent humidification. We have been reported that a variety of drug compounds could be adsorbed in mesoporous silicas by sealed-heating method.[13—15] When mefenamic acid, which is one of the anti-inflammatory drugs, was sealed-heated with a mesoporous silica FSM-16, color of the sample changed from white to blue. Effect of pore size of FSM-16 on coloration phenomenon and the molecular states of mefenamic acid and FSM-16 were investigated by solid-state NMR spectrometry.

Experimental

Materials Mefenamic acid (MFA), the structure of which is shown in Fig. 1, was obtained from Wako Pure Chemical Industries Ltd. (Osaka, Japan). Mefenamic acid has been reported to have two crystalline modifications: a stable polymorph I and a metastable polymorph II.[16,17] The MFA obtained was stable form I and used without further purification. Mesoporous silica FSM-16 (Oc) and FSM-16 (Doc) were kindly supplied by Toyota Central R&D Labs., Inc., Japan. Mean pore width and specific surface area of FSM-16 (Oc) and FSM-16 (Doc) were 16.0 and 45.0 Å, and 700 and 1040 m^2/g, respectively. FSM-16 was ground by mortar and pestle, sieved using a 125 μm aperture size sieve, and dried at 120 °C for 3 h under reduced pressure before use. All other chemicals were of reagent grade.

Abbreviations of quaternary ammonium surfactants used in the synthesis process are indicated by the initials (Oc) and (Doc) which are as follows: (Oc), *n*-octyl trimethyl ammonium bromide (or chloride); (Doc), *n*-dococyl trimethyl ammonium bromide (or chloride).

Preparation of Physical Mixture (PM) Physical mixture was prepared by mixing of MFA and FSM-16 at the weight ratio of 3 : 7 (MFA : FSM-16) in a glass vial for 1 min.

Preparation of Sealed-Heated Sample (SH) A MFA/FSM-16 PM (*ca.* 300 mg) was sealed in a glass ampoule (20 ml) and then heated at 140 °C for 5 h.

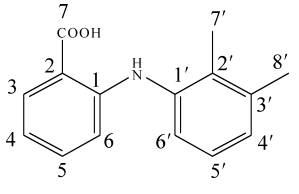

Fig. 1. Chemical Structure of MFA

* To whom correspondence should be addressed. e-mail: moribe@p.chiba-u.ac.jp

Preparation of Humidified Sealed-Heated Sample (HU-SH) A MFA/FSM-16 SH was humidified at 40 °C and 82% relative humidity (RH) for 3 months using potassium chloride saturated aqueous solution.

Colorimetric Measurement Powder sample was filled in a sample folder (PSH-001, JEOL, Japan). The color of the powder was measured by a reflectance method using FP-6500 spectrofluorometer (JEOL, Japan) equipped with integration sphere (ISF-153, JEOL, Tokyo, Japan) in the wavelength range of 380—780 nm. Reflectance of Spectralon® white standard plate was used for the calibration. The reflectance curve was digitalized using a color diagnostics program (JASCO V-500, JEOL, Japan) and the data were shown using L*a*b* color system.

Powder X-Ray Diffraction (PXRD) Powder X-ray diffraction measurement was conducted on a Rigaku Miniflex Powder X-ray diffractometer (Tokyo, Japan). The measurement conditions were as follows: target, Cu$K\alpha$; filter, Ni; voltage, 30 kV; current, 15 mA; scanning range, $2\theta=3$—35°; scanning speed, 4°/min.

Thermogravimetry (TG) Thermogravimetry was performed on the EXSTAR6000 TG/DTA6200 (SII Nanotechnology, Japan). The operating conditions were as follows: open-aluminum pan; sample weight, 5 mg; heating rate, 2 °C/min; temperature range, 30—300 °C; and nitrogen gas flow rate, 60 ml/min. In the case of MFA/FSM-16 SH and HU-SH, platinum pan was used with the heating rate of 2 °C/min at the temperature range of 30—1000 °C.

Solid-State ^{13}C-NMR Spectroscopy ^{13}C-NMR spectra were determined on a JNM-ECA600 (14.1 T) spectrometer (JEOL, Japan) operating with a pulse saturated transfer/magic angle spinning (PST/MAS) probe. The sample was filled in a cylindrical rotor and spun at 15 kHz. The measurement conditions were as follows: contact time, 5 ms; repetition time, 2 s; number of data points, 2048; number of accumulations, 1000—12000 times; external standard, adamantane.

Solid-State ^{29}Si-NMR Spectroscopy Solid-state ^{29}Si-NMR spectra were recorded using the apparatus mentioned above at a same magnetic field strength. ^{29}Si-NMR was measured using MAS with dipolar decoupling (^{29}Si-DD/MAS NMR). Polydimethylsilane was used as an external standard by adjusting the single peak to −34.0 ppm, which was measured by cross polarization (CP)/MAS method.

Results and Discussion

Adsorption and Coloration Behavior of MFA in FSM-16 Mesopores Sample appearances of MFA/FSM-16 (Oc) and MFA/FSM-16 (Doc) systems at the weight ratio of 3/7 are shown in Fig. 2. MFA was white- or pale yellow-colored crystals (Fig. 2a) and FSM-16 also white-colored powders (Figs. 2b, c). In MFA/FSM-16 (Oc), apparent color change was not observed by SH (Fig. 2e), though the color changed to bright blue in HU-SH (Fig. 2f). Color of the PM (Fig. 2h) of MFA/FSM-16 (Doc) changed from white to pale violet by the SH (Fig. 2i). The pale violet changed to deep one by the following humidification (HU-SH) (Fig. 2j). Coloration became deeper by using FSM-16 with larger pore size. On the contrary, coloration phenomena were not observed when the PM of MFA/FSM-16 (Doc) was humidified (Fig. 2k). These results indicated that adsorption of MFA in FSM-16 mesopores and the humidification deeply related to the coloration.

Powder X-ray diffraction patterns of unprocessed MFA crystals, MFA/FSM-16 PMs, SHs and HU-SHs are shown in Fig. 3. In the cases of PMs and MFA/FSM-16 (Oc) SH, the diffraction peaks of MFA crystals were clearly observed. The X-ray diffraction peaks were due to the MFA crystals remaining outside of the FSM-16 mesopores. In MFA/FSM-16 (Doc) SH and HU-SH, the diffraction peaks of MFA were not observed. These results indicate that most of MFA molecules were incorporated in FSM-16 (Doc) mesopores by the sealed-heating. Projected two-dimensional molecular size of MFA was reported as 6.1×9.9 Å (CS chem. 3D program).[18] In thermogravimetric measurement, MFA showed weight loss from 120 °C, even the mp of MFA was 231 °C, indicating the sublimable property of MFA. Since the pore size diameters of FSM-16 (Oc) and (Doc) were reported as 16.0 Å and 45.0 Å, respectively, it was possible that MFA molecules existed in the FSM-16 mesopores. Thus, it seems reasonable to expect that adsorption of MFA molecules in FSM-16 mesopores occurred through gaseous phase after the sublimation of MFA at 140 °C.

To investigate the color difference more precisely, colorimetric coordinate values of MFA/FSM-16 (Oc) and MFA/FSM-16 (Doc) represented by L*a*b* system were calculated and the results are shown in Fig. 4. Color can be presented using three elements: hue, chroma, and lightness. Hue, which is represented by the angle from a* axis in a*b* coordinate, is the property of colors by which they can be perceived as ranging from red through yellow, green, and blue, as determined by the dominant wavelength of the light. Chroma, which is represented by the distance from the origin in a*b* coordinate is the difference of a color against the brightness of another color which appears white under similar viewing conditions. Lightness (L*) is a property of a color, or a dimension of a color space, that is defined in a way to reflect the subjective brightness perception of a color for humans.[19] Figure 4 shows color difference of MFA, MFA/FSM-16 (Oc), and MFA/FSM-16 (Doc) represented by L*a*b* system. MFA was located on yellow-colored region in a*b* coordinate and FSM-16 (Oc) and (Doc) were located on colorless region close to origin. L* values of MFA and FSM-16 (Oc) and (Doc) were more than 85 %, indicated that these samples showed bright color. MFA/FSM-16 (Oc) SH was located on colorless region close to origin. On the other hand, deeply-colored MFA/FSM-16 (Doc) SH was located on blue-colored region. Chroma of MFA/FSM-16 HU-SH decreased compared with that of MFA/FSM-16 SHs due to the increased blue color. L* values of MFA/FSM-16 (Oc) and (Doc) SHs decreased compared with those of MFA and FSM-16. L* values of MFA/FSM-16 (Oc) and (Doc) HU-SHs further decreased compared with those of MFA/FSM-16 (Oc) and (Doc) SHs. Coordinate values of a* and b*, which determine hue and chroma of the sample, were almost same between MFA/FSM-16 (Oc) and MFA/FSM-16 (Doc) HU-SHs, though the L* value decreased with the increase of FSM-16 pore size. These results indicated that the color difference was mainly due to the difference of lightness.

Amount of MFA in FSM-16 Mesopores Amount of MFA adsorbed in FSM-16 mesopores was determined by TG measurement. Figure 5 shows thermogravimetric curves of MFA/FSM-16 (Oc) and MFA/FSM-16 (Doc) systems. Three steps in weight loss were observed in each curve. The first weight loss up to 100 °C was due to the release of adsorbed water. As the sublimation of intact MFA was observed between 120 °C and 300 °C, the weight loss observed in the range was caused by the sublimation of MFA which was not incorporated in mesopores. The weight loss observed at 300—1000 °C was expected to be due to MFA adsorbed in FSM-16 mesopores. Not only sublimation but also degradation of MFA in FSM-16 mesopores might occur on the process of heating. The TG curves observed were almost same between SH and HU-SH in both MFA/FSM-16 (Oc) and MFA/FSM-16 (Doc) systems. Humidification did not affect the amount of MFA in FSM-16 mesopores. It is assumed that the difference in the degree of lightness shown in Fig. 2

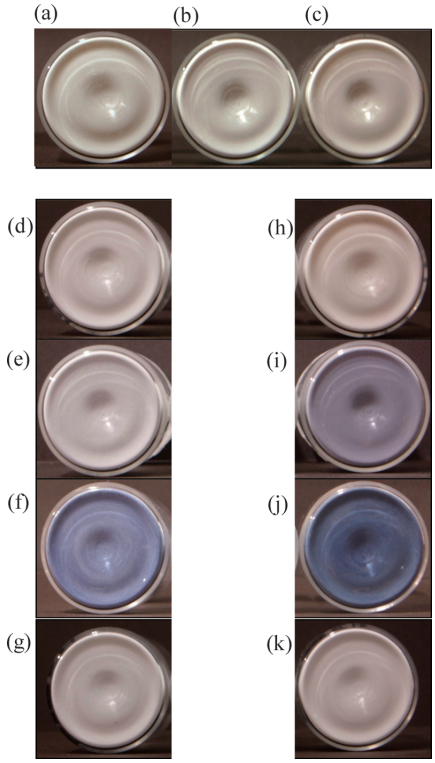

Fig. 2. Sample Appearances of MFA/FSM-16 (Oc) and MFA/FSM-16 (Doc) System

(a) MFA, (b) FSM-16 (Oc), (c) FSM-16 (Doc), (d) MFA/FSM-16 (Oc) PM, (e) MFA/FSM-16 (Oc) SH, (f) MFA/FSM-16 (Oc) HU-SH, (g) humidified MFA/FSM-16 (Oc) PM, (h) MFA/FSM-16 (Doc) PM, (i) MFA/FSM-16 (Doc) SH, (j) MFA/FSM-16 (Doc) HU-SH, and (k) humidified MFA/FSM-16 (Doc) PM.

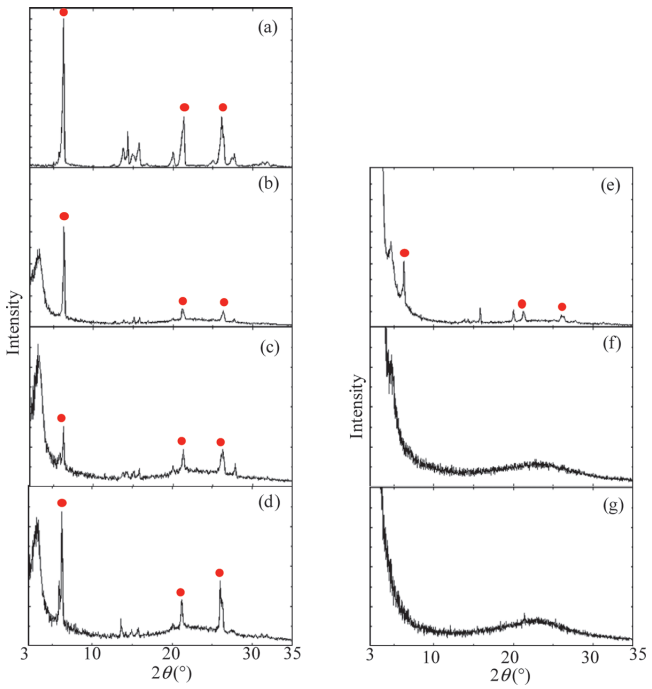

Fig. 3. PXRD Patterns of MFA/FSM-16 (Oc) and MFA/FSM-16 (Doc) System

(a) MFA, (b) MFA/FSM-16 (Oc) PM, (c) MFA/FSM-16 (Oc) SH, (d) MFA/FSM-16 (Oc) HU-SH, (e) MFA/FSM-16 (Doc) PM, (f) MFA/FSM-16 (Doc) SH, and (g) MFA/FSM-16 (Doc) HU-SH. ●: MFA.

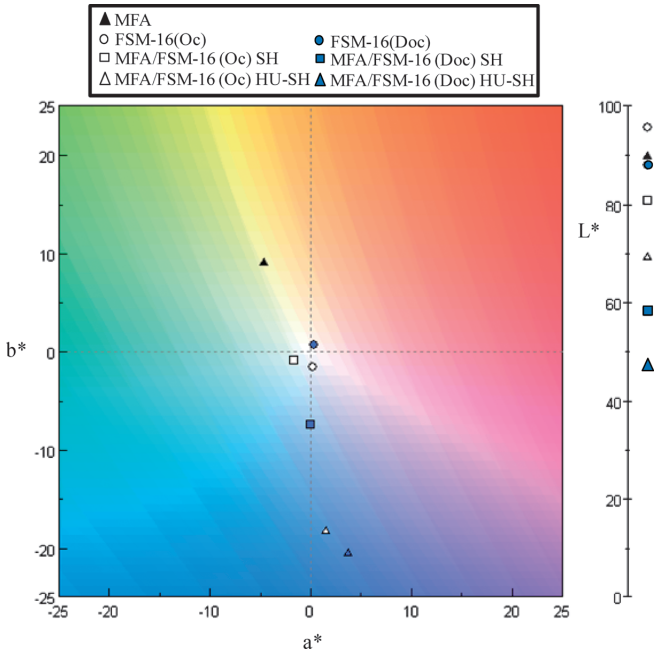

Fig. 4. Colorimetric Coordinate of MFA/FSM-16 (Oc) and MFA/FSM-16 (Doc) Represented by L*a*b* System

could be due to the difference of the adsorbed amount of MFA.

For HU-SHs, the amount of MFA adsorbed in FSM-16 mesopore was calculated and the results are shown in Table 1. The amount of MFA in the mesopore was found as 5.3±0.7 and 20.8±1.2% in MFA/FSM-16 (Oc) and MFA/FSM-16 (Doc) HU-SH, respectively. The incorporation efficiency (%), which was demonstrated by the amount of MFA adsorbed divided by total amount of MFA, was calculated as 16.4±1.7 and 72.7±2.8% in MFA/FSM-16 (Oc) and MFA/FSM-16 (Doc) HU-SH, respectively. It was found that the amount of MFA adsorbed in mesopores increased with an increase of the pore size.

Molecular States of MFA Evaluated by ^{13}C-Solid-State NMR ^{13}C-solid-state NMR measurement was performed to evaluate the molecular states of MFA in FSM-16 mespores. All spectral peaks were assigned from carbon atoms of MFA because FSM-16 did not contain carbon atoms. PST/MAS NMR spectra can detect carbon atoms with relatively high mobility, compared with cross polarization CP/MAS NMR spectra, which has been commonly used to evaluate molecular states of drugs. Molecular mobility of drug incorporated in mesoporous materials became high compared with the crystalline states.[20] Figure 6 shows ^{13}C-PST/MAS NMR spectra of MFA/FSM-16 SHs and HU-SHs. Crystalline MFA did not show any peak in this spectral region because of the low mobility (data not shown). In MFA/FSM-16 (Oc) SH, small new peaks were observed. In the spectrum of MFA/FSM-16 (Doc) SH, other new peaks, which were not observed in MFA/FSM-16 (Oc) HU-SH, were observed. The peak positions observed in the spectrum of MFA/FSM-16 (Doc) HU-SH were slightly different from those of MFA/FSM-16 (Doc) SH. Thus, molecular state of MFA in FSM-16 (Doc) mesopores could be changed by the humidification.

Molecular States of FSM-16 Evaluated by ^{29}Si-

Table 1. Incorporation Efficiency of MFA in Mesopores of FSM-16

	MFA not incorporated in FSM-16 (%)[a] (Weight loss: 100—300 °C)	MFA incorporated in FSM-16 (%)[a] (Weight loss: 300—1000 °C)	Total amount of MFA (%)[a] (Weight loss: 100—1000 °C)	Incorporation efficiency (%)[a]
MFA/FSM-16 (Oc) HU-SH	26.9±1.8	5.3±0.7	32.1±2.2	16.4±1.7
MFA/FSM-16 (Doc) HU-SH	7.8±0.9	20.8±1.2	28.0±1.6	72.7±2.8

a) All data are expressed as mean±standard deviation (n=3). *b*) Incorporation efficiency (%) = $\frac{\text{amount of MFA incorporated in FSM-16 (\%)}}{\text{total amount of MFA (\%)}} \times 100$.

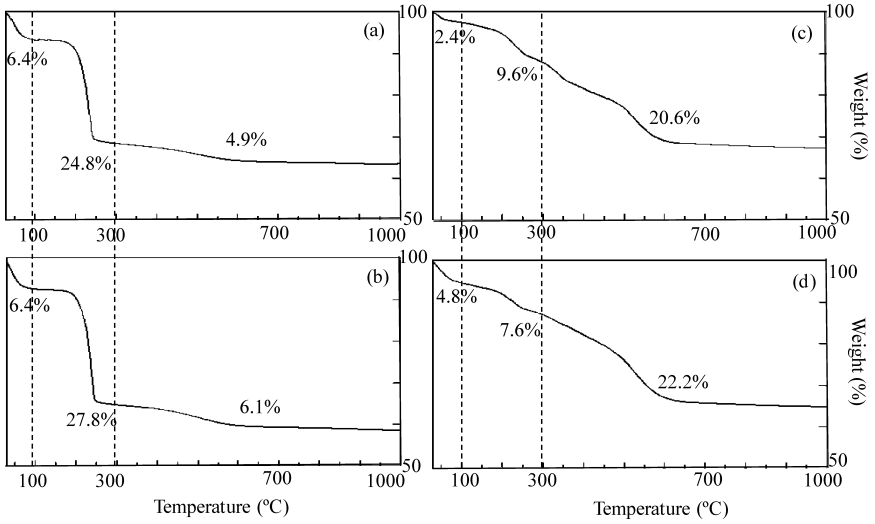

Fig. 5. Thermogravimetric Curves of MFA/FSM-16 (Oc) and MFA/FSM-16 (Doc) System

(a) MFA/FSM-16 (Oc) SH, (b) MFA/FSM-16 (Oc) HU-SH, (c) MFA/FSM-16 (Doc) SH, and (d) MFA/FSM-16 (Doc) HU-SH. Heating rate: 5 °C/min.

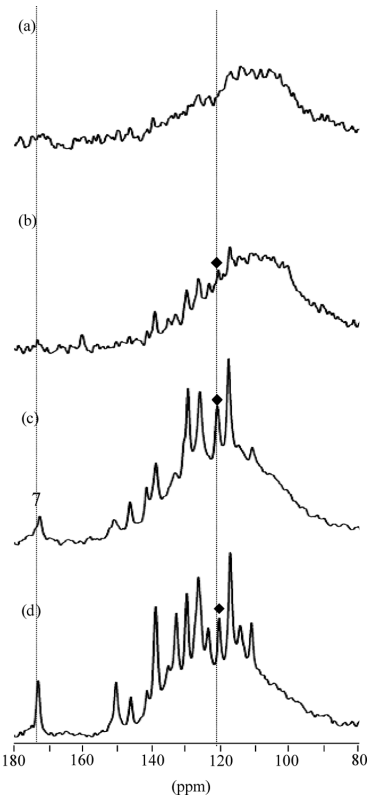

Fig. 6. ^{13}C-PST/MAS NMR Spectra of MFA/FSM-16 System

(a) MFA/FSM-16 (Oc) SH, (b) MFA/FSM-16 (Oc) HU-SH, (c) MFA/FSM-16 (Doc) SH, and (d) MFA/FSM-16 (Doc) HU-SH. ◆: new peak.

DD/MAS NMR ^{29}Si-DD/MAS NMR spectra of FSM-16 (Doc) before and after the humidification were compared (Fig. 7). Peaks observed in ^{29}Si-NMR spectrum are known due to Si atom with two hydroxyl groups (Q2, geminal silanol, *ca.* 90 ppm), that with one hydroxyl group (Q3, single silanol, *ca.* 100 ppm) and that with no hydroxyl group (Q4, siloxane, *ca.* 110 ppm).[21—23] In the ^{29}Si-DD/MAS NMR spectrum before humidification, two peaks assigned to Q3 and Q4 were observed. Additional small peak of Q2 appeared after the humidification, indicating that the humidification induced the increase of geminal silanol groups.

Molecular states of MFA/FSM systems before and after humidification were evaluated by ^{29}Si-DD/MAS NMR (Fig. 8). Only the two peaks assigned to Q3 and Q4 were observed in MFA/FSM-16 (Oc) and (Doc) SHs before humidification. On the other hand, a Q2 peak in addition to Q3 and Q4 was observed in MFA/FSM-16 (Oc) and (Doc) HU-SHs. These results indicated that geminal silanol groups in FSM-16 (Oc) and (Doc) was produced by the humidification regardless of the pore size and the presence of MFA. Tatsumi *et al.* reported that the Q2 component, which was observed by the humidification of moseporous silica MCM-48, was increased by hydrolysis of Si–O–Si siloxane bonding and the subsequent increase of Si–OH groups.[24] Similar phenomenon should be occurred in FSM-16. Furthermore, the increase of hydroxyl groups on the FSM surface by the humidification affected on the molecular states of MFA molecules adsorbed in FSM-16 mesopores. It was presumed that the coloration of MFA/FSM-16 by HU-SH was caused by the change of molecular states of MFA in FSM-16 through the increase of hy-

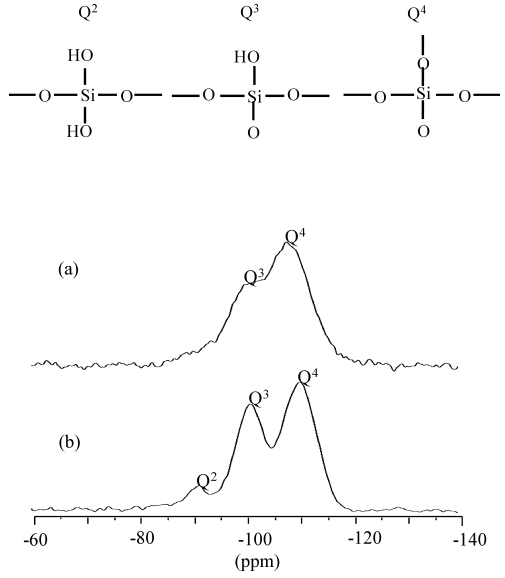

Fig. 7. Changes in ^{29}Si-DD/MAS NMR Spectra of FSM-16 (Doc) (a) before and (b) after Humidifying at 40 °C and 82% RH for 3 Months

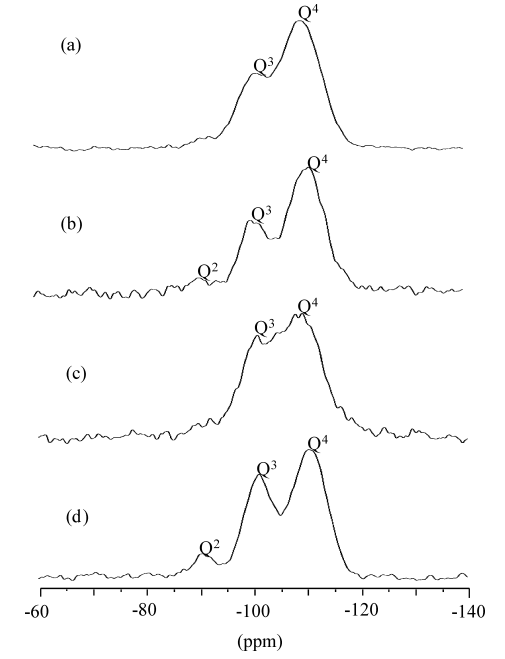

Fig. 8. ^{29}Si-DD/MAS NMR Spectra of MFA/FSM-16 System

(a) MFA/FSM-16 (Oc) SH, (b) MFA/FSM-16 (Oc) HU-SH, (c) MFA/FSM-16 (Doc) SH, and (d) MFA/FSM-16 (Doc) HU-SH.

droxyl groups on FSM surface by humidification.

Following two coloration mechanism are currently hypothesized from this study: Structure of MFA molecules were changed by intramolecular proton transfer activated by the increase of Si–OH groups. We speculated that the elongation of conjugate double bonds and the presence of OH groups on the edges induced the long-wavelength shift of MFA, which caused blue coloration. Another mechanism was proposed from the results of PST/MAS NMR spectra. We speculated that increased π–π stacking interactions among MFA molecules in FSM-16 mesopores correlated to the long-wavelength shift.

Conclusion

Mefenamic acid could be incorporated in FSM-16 mesopores by sealed-heating treatment. Coloration of MFA by the adsorption in FSM-16 changed depending on the pore size. In the case of MFA/FSM-16 (Doc), the color of SHs was changed from pale violet to brilliant blue by the subsequent humidification. Different incorporated amount of MFA in FSM-16 affected the coloration caused by the changes of chroma and lightness. Molecular mobility of MFA was increased not only by the incorporation into mesopores but also the subsequent humidification. The changes of the molecular state of MFA induced the coloration phenomenon. The coloration phenomena were also observed by SH of MFA and humidified FSM-16. Changes of the molecular states of FSM-16 by HU as well as MFA adsorption in FSM-16 mesopore by SH affected the coloration.

Acknowledgement We wish to express our thanks to Toyota Central R&D Labs., Inc., Japan for provision of FSM-16.

References

1) Maniwa Y., Masubuchi S., Minamisawa T., Kira H., Kodaira T., Kazama S., *Chem. Phys. Lett.*, **424**, 97—100 (2006).
2) Georg A., Graf W., Neumann R., Wittwer V., *Solid State Ionics*, **127**, 319—328 (2000).
3) Son Y., Park Y., Park S., Shin C., Kim S., *Dyes Pigments*, **73**, 76—80 (2007).
4) Shirai K., Matsuoka M., Fukunishi K., *Dyes Pigments*, **47**, 107—115 (2000).
5) Shirai K., Matsuoka M., Matsumoto S., Shiro M., *Dyes Pigments,* **56**, 83—87 (2003).
6) Sheth A. R., Lubach J. W., Munson E. J., Muller F. X., Grant D. J., *J. Am. Chem. Soc.*, **127**, 6641—6651 (2005).
7) Abe T., Itakura T., Ikeda N., Shinozaki K., *Dalton Trans.*, **4**, 711—715 (2009).
8) Kojima T., Onoue S., Katoh F., Teraoka R., Matsuda Y., Kitagawa S., Tsuhako M., *Int. J. Pharm.*, **336**, 346—351 (2007).
9) Pongpeerapat A., Higashi K., Tozuka Y., Moribe K., Yamamoto K., *Pharm. Res.*, **23**, 2566—2574 (2006).
10) Tishmack P. A., Bugay D. E., Byrn S. R., *J. Pharm. Sci.*, **92**, 441—474 (2003).
11) Berendt R. T., Sperger D. M., Isbester P. K., Munson E. J., *Trends Anal. Chem.*, **25**, 977—984 (2006).
12) Nelson B. N., Schieber L. J., Barich D. H., Lubach J. W., Offerdah T. J., Lewis D. H., Heinrich J. P., Munson E. J., *Solid State Nucl. Mag.*, **29**, 204—213 (2006).
13) Tozuka Y., Oguchi T., Yamamoto K., *Pharm. Res.*, **20**, 926—930 (2003).
14) Tozuka Y., Sasaoka S., Nagae A., Moribe K., Oguchi T., Yamamoto K., *J. Colloid Interface Sci.*, **291**, 471—476 (2005).
15) Tozuka Y., Wongmekiat A., Kimura K., Moribe K., Yamamura S., Yamamoto K., *Chem. Pharm. Bull.*, **53**, 974—977 (2005).
16) Gilpin R. K., Zhou W., *J. Pharm. Biomed. Anal.*, **37**, 509—515 (2005).
17) Aguiar A. J., Zelmer J. E., *Pharm. Res.*, **8**, 983—987 (1969).
18) Del Arco M., Fernández A., Martín C., Rives V., *Appl. Clay Sci.*, **36**, 133—140 (2007).
19) Siddiqui A., Nazzal S., *Int. J. Pharm.*, **341**, 173—180 (2007).
20) Azaïs T., Tourné-Péteilh C., Aussenac F., Baccile N., Coelho C., Devoisselle J. M., Babonneau F., *Chem. Mater.*, **18**, 6382—6390 (2006).
21) Léonardelli S., Facchini L., Fretigny C., Tougne P., Legrand A. P., *J. Am. Chem. Soc.*, **114**, 6412—6418 (1992).
22) Koyano K. A., Tatsumi T., Tanaka Y., Nakata S., *J. Phys. Chem. B*, **101**, 9436—9440 (1997).
23) Antochshuk V., Jaroniec M., *J. Phys. Chem. B*, **103**, 6252—6261 (1999).
24) Tatsumi T., Koyano K. A., Tanaka Y., Nakata S., *Chem. Lett.*, **26**, 469—470 (1997).